SPECIAL TOPICS — Acoustics

Research on the acoustic scattering function and coherence properties from rough seafloor based on finite element model*

Bo Lei(雷波), Yi-Xin Yang(杨益新)†, Yuan-Liang Ma(马远良), and Dong-Xu Chen(陈东旭)

School of Marine Science and Technology, Northwestern Polytechnical University, Xi'an 710072, *China*

(Received 25 July 2016; revised manuscript received 27 September 2016; published online 25 October 2016)

Acoustic scattering from a rough sea bottom is recognized as a main source of reverberation. In this study, scattering properties from a layered bottom were exploited based on the finite element model. The scattering strength and loss from the layered rough seabed were investigated by ensembling the realizations of rough interface. They were found to be dependent on the thickness of sediment, and interference was significant in the case of thin sediment. Through verification of the finite element model, the scattering loss could be evaluated using the Eckart model with a proper sound speed in the thick sediment. The multiple scattering effect on the sound field was also exploited. It revealed that the effect depended strongly on the bottom type.

Keywords: finite element, rough seafloor, scattering function, coherence

PACS: 43.30.Hw **DOI:** 10.1088/1674-1056/25/12/124312

1. Introduction

Over the past decades, acoustic scattering by rough seafloor has been recognized as a significant source of reverberation. For this reason, accurate models that help to make sense of the interaction of acoustic waves with the sea bottom are necessary. As a particular source, seafloor roughness can be a dominant contributor to sound scattering at higher frequencies.

Quantifying the effects of surface roughness on the pressure field scattered from the seafloor has been extensively exploited. Scattering problems are solved with theoretical models by making various assumptions in approximating the Helmholtz–Kirchhoff (HK) integral. The three well-known models are perturbation theory (PT)[1,2] in which the scattered pressure is expanded in a Taylor series; Kirchhoff approximation (KA)[3] in which the pressure and its normal derivative are calculated analytically from the incident pressure; and the hybrid model called small slope approximation (SSA),[4,5] which combines KA (most effective near the specular angle) and PT (more accurate away from specular).

Some possible solutions from layered rough bottom scattering were further introduced into scattering. Kuperman[6] presented a self-consistent PT-to-rough-surface scattering in stratified media by introducing a boundary condition operator. Ivakin[7] studied the first-order solutions for stratified fluid sediments with an arbitrary number of interfaces, and the bottom bistatic scattering strength in the form of auto- and cross-spectra of the roughness of the different interfaces. Thorsos *et al.*[3] discussed the validity of the PT method by comparison with solving an integral equation and higher-order prediction. Jackson[8] combined the KA model with the first-order PT model for scattering on very rough seafloors over the low-frequency and mid-frequency range.

The approximations in these common methods do not generally include the effects of multiple scattering or shadowing. The finite element (FE) model could provide an approximate solution to boundary-value problems, approaching the exact solution of the Helmholtz function with finer elements. It can also include all the effects that are not limited to the boundary, such as layers and gradients, with the disadvantage of computation cost. It is more attractive with the development of computation technology. Isakson *et al.*[9,10] proposed an FE method to model the acoustic scattering on the fluid and elastic interface between two half spaces, which provides a good solution. Furthermore, the FE model can serve to benchmark approximate models and provide a way to study non-boundary effects.

Over the stratified sea bottom, the multiple scattering between interfaces is possibly significant. This paper aims to study the scattering properties, including scattering function and reflection loss on the rough seafloor, by considering layering and gradients. The built FE models are similar to those in the work of Isakson. The reflection loss and backscattering strength on the rough seafloor is analyzed and compared with the KA-based model. Furthermore, multiple scattering in a shallow water environment is studied based on FE as a benchmark. The spatial coherence of the total field is analyzed.

The rest of this paper is organized as follows: Section 2

*Project supported by the National Natural Science Foundation of China (Grant No. 61571366), the Natural Science Basic Research in Shaanxi Province of China (Grant No. 2015JQ5199), and the Fund of Science and Technology from the Underwater Test and Control Laboratory (Grant No. 9140c260201130c26096).

†Corresponding author. E-mail: yxyang@nwpu.edu.cn

© 2016 Chinese Physical Society and IOP Publishing Ltd

presents the FE models for scattering on the rough seafloor and Section 3 provides results on reflection loss and scattering strength. Section 4 presents multiple scattering in a shallow environment as a benchmark to examine the spatial coherence of the acoustic field. Section 5 provides a summary of the paper.

2. Scattering from rough seafloor

When a plane wave is incident on a rough interface, scattering and transmission occur. For ocean sediment, the roughness spectra of an isotropous rough interface have been shown to satisfy power-law statistics rather than Gaussian.[8] However, a pure power law would be unphysical infinite at a spatial wavenumber of zero. Therefore, the interface of the sea bottom is usually characterized by a von Karman spectral in the form of

$$W(K) = \omega / \left(K_L^2 + K^2\right)^{\gamma/2}, \tag{1}$$

where K is the spatial wave number, K_L is the cutoff wavenumber, ω denotes the spectral strength, and γ is the spectral exponent. The case studied in this paper is in two dimensions; thus, the one-dimensional (1D) form of the von Karman spectral is used. The root-mean-square roughness h could be calculated with the relationship between the 1D and two-dimensional (2D) forms of the von Karman spectral.[11]

The FE model is expected to be the most accurate with the computational domains discretized into a finite number of elements. A weak formulation of a given partial differential equation (PDE) is derived and assembled to a global linear equation, thereby generating a solution. If the discretization of grids is sufficiently fine, an FE solution converges to the exact solution. The domains in Fig. 1 are discretized into unstructured triangular elements. The PDEs are solved on each of these elements by using a quadratic Lagrange polynomial basis set. The size of elements in the computation domain is empirically suggested to be less than $\lambda/6$, where λ is the wavelength in the domain, and with a much smaller size near the rough interface. The coefficients of each of the basis set polynomials in each of the elements are solved using a variational equation through the Galerkin method.[12] A multifrontal massively parallel spaces (MUMPS) direct solver[13] is used. All the meshing, solving, and postprocessing procedures are realized in the commercial code COMSOL.[14]

The scattering problem is infinite in reality. However, the finite domain is expected because of the computational burden. Thus, boundary reflections have to be effectively reduced or eliminated. This is performed by using well-known perfectly matched layers (PMLs)[15–17] in the scattering problem. PMLs transform the spatial coordinates into complex coordinates such that the medium is dissipative in a particular direction. In this study, rectangular PML surrounding a fluid domain is considered, as shown in Fig. 1. The thickness of the PML is set to 0.75 m to ensure well-reduced boundary reflection.

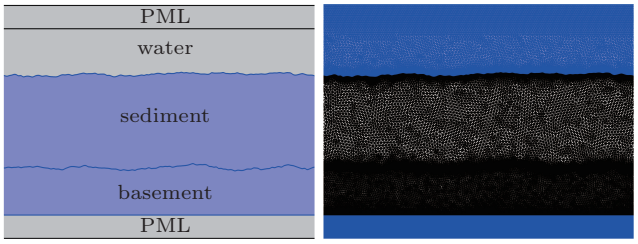


Fig. 1. (color online) FE model of rough interface scattering in two dimensions. The three-layered environment is separated by the two rough interfaces. PMLs around the computation domains are used to avoid the reflection from computation boundaries.

Owing to the finite extent length of the rough interface in the FE model, a Gaussian tapered plane wave approximation is used with a beam waist being a quarter of the interface length, resulting in approximate zero incident strength on the model edges. Therefore, the diffraction effect from the model edge could be avoided. In most cases, the interface length is set to be 80 λ. When the incident grazing angle is lower than 10°, Kapp proposed a beam waist criterion to reduce the undesirable curvature in the incidence.[18] For the scattering calculation at very shallow angles, a larger interface length is required in the FEM models, leading to a high computation cost.

After these procedures, the pressure and its normal derivatives are calculated. Then, the far field pressure at the receiver is computed using the 2D form of the HK integral, and the Green function is substituted by the Hankel function in the far field, thereby yielding

$$p_s(\boldsymbol{r}) = \frac{1}{4\mathrm{i}} \int_s \left[p_s(\boldsymbol{r}_s) \cdot \mathrm{i}k \cdot \frac{\boldsymbol{r} - \boldsymbol{r}_s}{|\boldsymbol{r} - \boldsymbol{r}_s|} \cdot \boldsymbol{n} - \frac{\partial p_s(\boldsymbol{r}_s)}{\partial \boldsymbol{n}} \right] \times \sqrt{\frac{2}{\pi k}}\, \mathrm{e}^{\mathrm{i}\pi/4} \frac{\mathrm{e}^{-\mathrm{i}kr}}{\sqrt{r}}\, \mathrm{e}^{\mathrm{i}k_s r_s}\, \mathrm{d}s, \tag{2}$$

where $p_s(\boldsymbol{r}_s)$ is the scattered pressure on the interface position $\boldsymbol{r}_s$, $\boldsymbol{r}$ is the receiver position at the scattered angle θ_s, $r = |\boldsymbol{r}|$, and $\boldsymbol{n}$ is the outward normal direction on the interface.

As an important factor in propagation, the coherent reflection loss could be calculated using the ratio of the coherent mean of the scattered pressure at the specular direction from the rough interface to that of a flat pressure release surface, expressed as

$$RL_{\mathrm{coh}}(\theta) = 10 \log_{10} \left(\frac{|\langle P_{\mathrm{rou}}(\theta) \rangle|^2}{\left| P_{\mathrm{flat_PR}}(\theta)^2 \right|} \right), \tag{3}$$

where θ is the grazing angle of the incident wave, and P_{rou} and $P_{\mathrm{flat_PR}}$ are the scattering pressure at the far field with the rough bottom interface realization and press release flat interface, respectively.

Scattering strength, another metric factor on the non-specular direction, is considerable in reverberation. Once the

pressure at the receiver is determined, the scattering cross section at the grazing angle θ can be computed using the following expression:[9]

$$\sigma(\theta) = \left\langle |p_s(\boldsymbol{r}(\theta))|^2 \right\rangle r \Big/ \left(\sqrt{\frac{\pi}{2}} g \right), \tag{4}$$

where g is the beam waist and the range r is set to be 100 m. Consequently, the scattering strength is the logarithm of the cross section in decibels.

3. Scattering properties on rough seafloor

A three-layered underwater environment was considered, as shown in Fig. 1. A half-space basement is covered with sediment. The upper interface (between water and sediment) and lower interface (between sediment and basement) is assumed to be rough, as described by the von Karman spectral. The acoustic parameters are shown in Table 1. The acoustic parameters on the top of the sediment are the same as those in the SwellEx-96[19] experiment. The two interfaces have the same roughness parameters, with $\omega = 0.0008$ m$^{3-\gamma}$, $K_L = 0.5$ m^{-1}, $\gamma = 2$, and the root-mean-square roughness height $h = 0.071$ m. 60 realizations are independently generated according to the von Karman spectral. A sound frequency of 2 kHz leads to $h/\lambda = 0.0947$. The fluid and elastic basements are considered. On the upper and lower interfaces, the critical angle is approximately 17° and 33°, respectively.

The thickness of the sediment is assumed to be 3 m, and the reflection loss at different grazing angles are computed with the FE model according to Eq. (3). The statistical reflection loss is shown in Fig. 2. To study the scattering effects on the rough interface, the analytical results from flat interfaces are compared. In Fig. 2(a), the two results are almost the same at a grazing angle lower than 20°. The reflection loss is apparent at the grazing angles lower than the critical angle 17° because the evanescent waves penetrate into the seafloor according to wave motion theory. A slight difference is present between the two results, due to the roughness contribution to the transmission of incident waves. When the grazing angle increases, the reflection loss on the rough interface is approximately 3 dB stronger than the flat one because of the contribution from roughness-induced scattering. Once the incident and specular direction are closed, the roughness-induced scattering is more significant, and a difference of almost 6 dB is observed relative to flat interface reflection. In other words, the scattering contribution on the forward direction could be ignored at a very low grazing angle, while scattering plays an important role at a large grazing angle. Although the reflection loss pattern with elastic basement shown in Fig. 2(b) exhibits different values, the roughness-induced scattering presents a similar effect.

Table 1. Parameters in the model.

Parameters	Value
Sea water	
Sound speed	1500 m/s
Density	1000 kg/m^3
Sediment	
Upper sound speed	1572 m/s
Density	1760 kg/m^3
Attenuation	0.314 dB/λ
Fluid basement	
Sound speed	1881 m/s
Density	2060 kg/m^3
Attenuation	0.113 dB/λ
Elastic basement	
Compressional sound speed	2550 m/s
Shear sound speed	1050 m/s
Density	2600 kg/m^3
Compressional attenuation	0.096 dB/λ
Shear attenuation	0.3 dB/λ

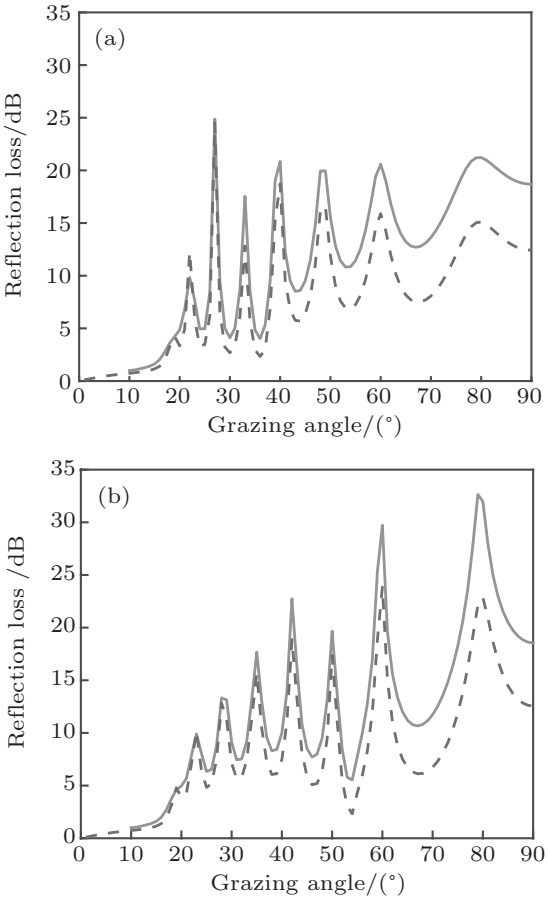


Fig. 2. Reflection loss from rough seafloor. Panel (a) is with fluid basement and panel (b) is with elastic basement. The FE model with rough interfaces (solid line) and analytical solution with flat interfaces (dash line) are compared.

As another key property of the seafloor, backscattering could cause significant reverberation from the rough interface. The backscattering strength is shown in Fig. 3. The backscattering strength has a Lambert-like angular dependence. At

a lower angle, the backscattering strength is approximately −25 dB and increases to approximately 0 dB at 90°. Results from different thickness sediments are compared. An obvious difference is observed at a low angle. At a grazing angle lower than 17° (critical angle on the upper interface), almost no wave could penetrate into the sediment, and the scattering occurs only on the upper interface; thus, backscattering is almost the same independent of the sediment thickness. At an angle range approximately from 17° to 33° (critical angle on the lower interface), the wave transmits into the sediment and then scatters on the lower interface, and the backscattering strength is the coherent summation of scattering from both interfaces. Meanwhile, the attenuation in the thinner sediment is weaker. Consequently, the construction and destruction interference are more significant from the thinner sediment. When the grazing angle exceeds approximately 37°, the small difference may be due to the slightly strong attenuation in the 3-m thickness sediment compared with that in the 1-m thickness sediment. If the basement is elastic, it exhibits a similar pattern, with slightly stronger backscattering at a grazing angle over 40° because of the high impedance of the basement.

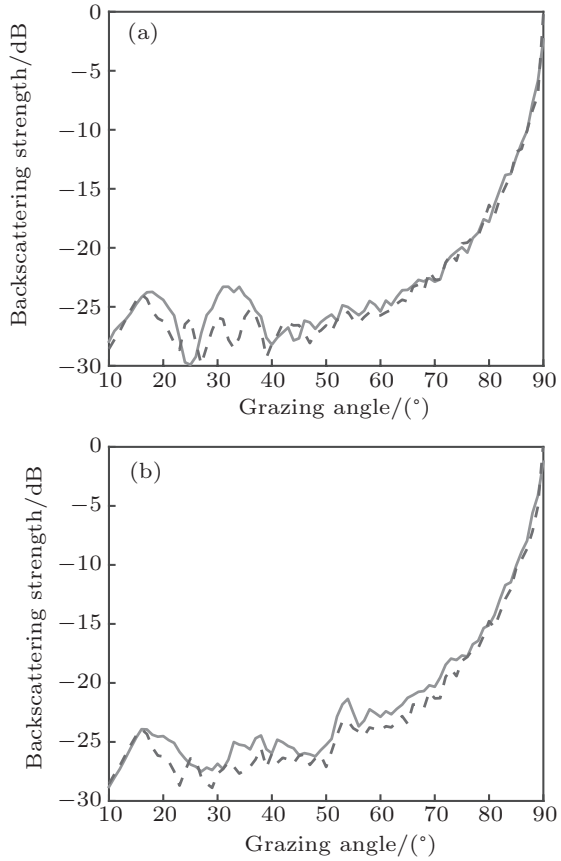


Fig. 3. Backscattering strength from rough seafloor with different sediment thickness. Panel (a) is with fluid basement and panel (b) is with elastic basement. The solid and dash lines indicate the sediments with 1 m and 3 m thickness, respectively.

In the case of thick sediment, the gradient of sound speed is present; thus, the interaction of sound with the seafloor is more complicated. As an example close to reality, the acoustic parameters of sediment in SWellEx are used. The sediment thickness is 23.5 m, and the sound speed on the upper and lower interface is 1572 m/s and 1593 m/s, respectively. Thus, the gradient of sound speed is 0.89 s^{-1}. Under this environment, the basement has a weak contribution to the rough interface scattering because of the extensive attenuation in the sediment. The KA-based models require isovelocity in the sediment. In this case, the error might be significant. The FE model provides an exact benchmark that could be used to verify the KA-based model. A KA-based model called the Eckart model[20] is analyzed. The sound speed on the seafloor is required in this model. Thus, two sound speed values corresponding to the one on the seafloor and the mean speed are considered. The computation results are shown in Fig. 4, in which the FE and Eckart models are compared. As shown in Fig. 4(a), the FE model has almost the same results as the Eckart model with seafloor sound speed at a low grazing angle, whereas it has similar results as the Eckart model with mean sound speed at a large grazing angle. Figure 4(b) exhibits the same results in the elastic case because the incidence interacts with the top volume of the sediment at a lower angle, resulting in reflection loss that is only dependent on the acoustic parameter near the top interface. At a higher angle, an excessive amount of energy penetrates deeply into the sediment, and reflection loss is a comprehensive effect of the sediment.

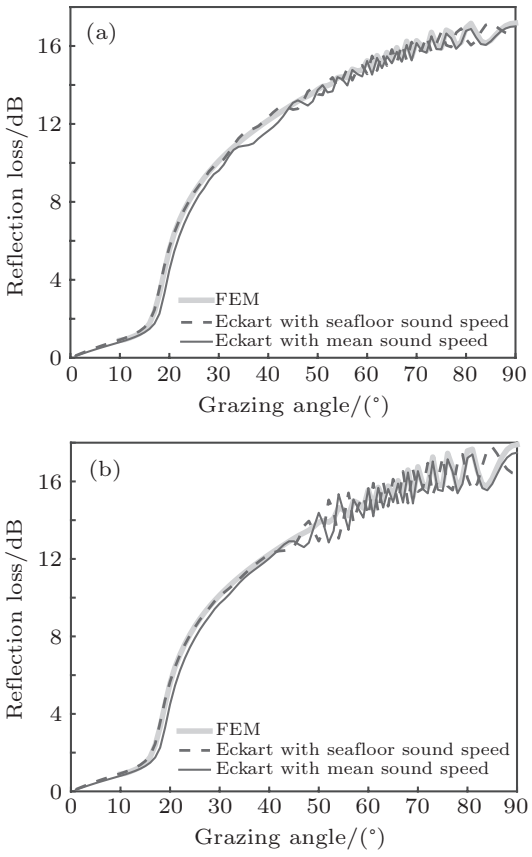


Fig. 4. Reflection loss from rough seafloor with gradient sound speed in the sediment. Panel (a) is with fluid basement and panel (b) is with elastic basement.

This finding indicates that the Eckart model could predict reflection loss with sound speed on the seafloor at a low grazing angle and with mean speed at a high grazing angle in the case of thick sediment.

4. Multiple scattering from rough seafloor

The wave interacts with the sea bottom when it propagates in shallow water, which may cause multiple scattering on the seafloor. As a further application of the FE concept, the multiple scattering in the littoral is exploited. Although the FE-based model entailed high computation cost, it could provide certain benchmarks for the multiple scattering in the waveguide. The FE-based model is illustrated in Fig. 5, with surrounding PMLs similar to the rough seafloor scattering. The cylindrical symmetrical boundary condition is satisfied at the source range. The roughness of the seafloor is generated according to von Karman spectral. A point source is deployed in the waveguide, and the entire domain is meshed into triangular elements. Consequently, the acoustic field is acquired with solver MUMPS in COMSOL.

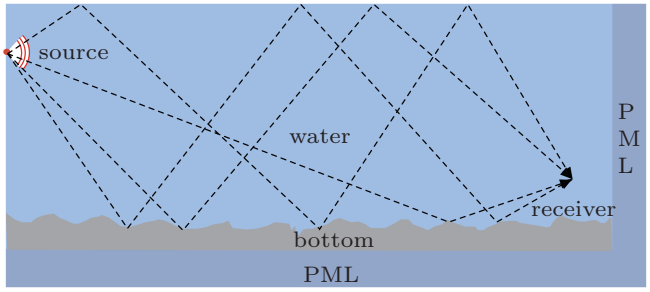


Fig. 5. (color online) Multiple acoustic scattering in shallow water with rough seafloor.

In this study, statistical measures defined in Ref. [21] are used to show the energy distribution and coherence in space. The defined spatial correlation is the second moment expected value of the sound field at two receivers located at (x_1, z_1) and (x_2, z_2), and is expressed as

$$C(x_1, z_1, x_2, z_2) = \left\langle p(x_1, z_1)\, p(x_2, z_2)^* \right\rangle, \tag{5}$$

where p is the sound pressure and "*" indicates the complex conjunction. Indeed, the spatial correlation of the total acoustic field is widely used because the scattering field and mean field components cannot be received separately. The normalized correlation is further defined as

$$C_{Tij} = \frac{Re\left[C(x_1, z_1, x_2, z_2)\right]}{\sqrt{C(x_1, z_1, x_1, z_1) C(x_2, z_2, x_2, z_2)}}, \tag{6}$$

and the spatial coherence

$$\rho_{Tij} = \frac{|C(x_1, z_1, x_2, z_2)|^2}{C(x_1, z_1, x_1, z_1) C(x_2, z_2, x_2, z_2)}. \tag{7}$$

When the two receivers are placed at the same point, the spatial correlation is the expected intensity.

A typical shallow water environment is considered as a benchmark to exploit the effects of multiple scattering on the sound field. The water depth is assumed to be 50 m, and the acoustic parameters of the sediment are the same as in the previous example. The basement is elastic with the parameters shown in Table 1. The spatial coherence at 300 Hz is considered because of the limited computation resource. Two scenarios with fluid and elastic sediments are considered. To investigate the effect of roughness on the acoustic field, a larger mean square of the roughness is considered. In the following environment, $\omega = 0.008$ m$^{3-\gamma}$, $K_L = 0.1$ m^{-1}, and $\gamma = 2$ lead to $h = 0.5013$. However, the value of h/λ is still approximately maintained at 0.1.

The transmission loss at a depth of 40 m is shown in Fig. 6. In the flat interface, the transmission loss is calculated with the normal-mode model.[22] It shows that the transmission loss pattern, induced by roughness scattering, changes slightly except at the destruction interference range. In the fluid case, the higher-order modes are attenuated well in the far range, while in the elastic case, they are kept in the waveguide, and the lower-order modes are converted into shear waves in the sea bottom. Consequently, the averaged transmission loss in the second case is higher than that in the fluid one.

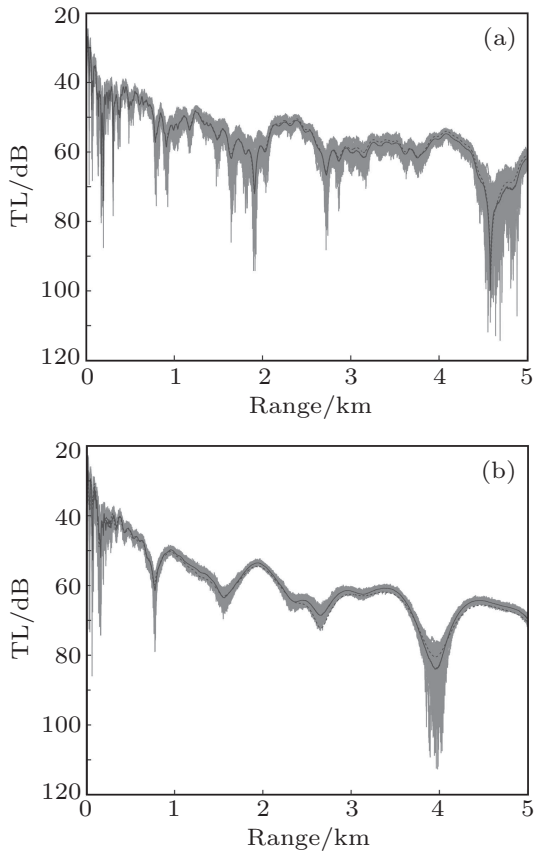


Fig. 6. Transmission loss in a shallow water environment. Receiver depth is 40 m. The solid and dash lines indicate the transmission loss from averaged FE results and from a flat interface environment, respectively. Panel (a) is fluid sediment and panel (b) is elastic.

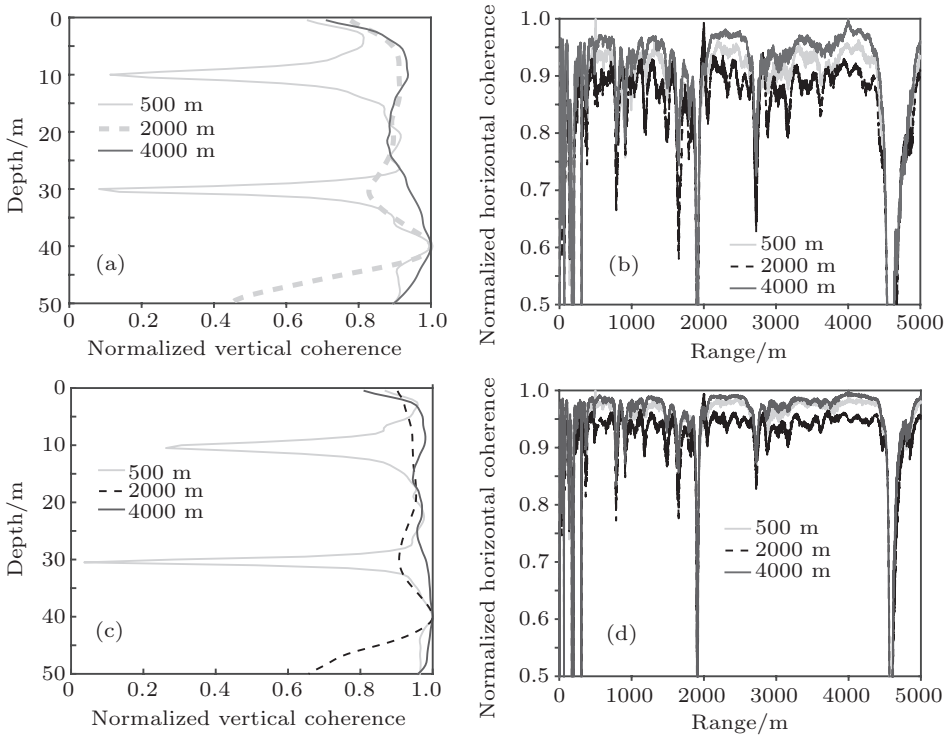


Fig. 7. Total field coherence in a fluid sediment case, at ranges of 500, 2000, and 4000 m. Receiver depth is 40 m. Panels (a) and (c) are vertical coherence, panels (b) and (d) are longitudinal coherence. The horizontal axes in panels (b) and (d) represent the range from the source to one receiver.

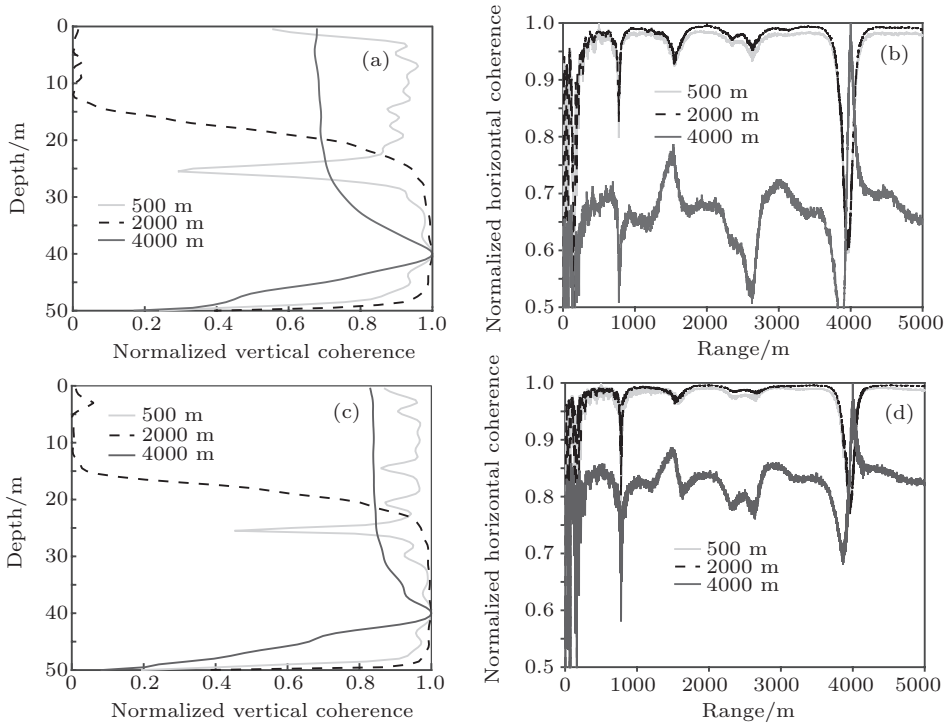


Fig. 8. Total field coherence in an elastic sediment case, at ranges of 500, 2000, and 4000 m. Receiver depth is 40 m. Panels (a) and (c) are vertical coherence, panels (b) and (d) are longitudinal coherence. The horizontal axes in panels (b) and (d) represent the range from the source to one receiver.

The vertical coherence and longitudinal coherence of the fluid scenario are shown in Fig. 7. In the fluid case, since the leaky modes in the incident field have been excited and are strong at the shorter range, the total field coherence has a narrow mainlobe. When the range increases, these higher-order modes are well attenuated, giving mainlobes roughly the same width and resulting in higher coherence. For comparison, the roughness h goes down to 0.22 ($K_L = 0.5$ m^{-1}), and the results are shown in Fig. 7(c) and 7(d). Obviously, both the vertical and longitudinal coherences are higher than those in

panels (a) and (b), due to the weaker scattering that happens on the rough seafloor. If no scattering occurs, the total field coherence is characterized by unity at all depths. It indicates that the total field coherence is strongly affected by the scattered field coherence in the short-range scale, and is close to unity in the far range. Notably, the longitudinal coherence has a much greater coherent length, and the longitudinal statistics are clearly shaped by modal interference lengths, as shown in Fig. 7(b).

Another scenario is that the sediment is elastic with the parameters presented in Table 1. The more interesting difference is observed in this case. Minimal radiation occurs in the bottom, so almost all scattered energy is trapped in the water column. As a result, the scattering field strength grows with range. Since the leaky modes have a strong effect on the spatial coherence, the effects of scattering are more obvious in this scenario. As shown in Fig. 8(a), the vertical coherence is above 0.9 at the 500 m range, while it degrades to 0.7 at the 4000-m range. Compared with Fig. 7, figure 8(a) reveals that the effects of scattering depend strongly on the bottom type. The case $h = 0.5013$ is considered as well. The vertical and longitudinal coherence are plotted in panels (c) and (d), respectively. Similar to in Fig. 7, the results are higher than in panels (a) and (b). When the interface become flat, no acoustic scattering occurs on the interface, hence the coherence will be unit.

5. Conclusions

Acoustic scattering from the rough sea bottom might have a significant effect on acoustic field properties. In this study, an FE-based scattering model is exploited for two-layered bottoms. The pressure and its normal derivative on a rough interface are calculated for an incident Gaussian-shaded plane wave. Scattering strength is calculated by using the HK integral and bottom loss in the specular direction, which proceeds in a manner similar to a flat interface for comparison. It should be emphasized that the results are the mean values at a point in the far field from an ensemble of rough interface realizations.

For the thin sediment, the results indicate that the reflections have peaks caused by multipath interference, and the reflection loss from scattering grows with the grazing angle for both of the two sediments. The backscattering strength has a Lambert-like angular dependence with significant interference from the two interfaces. Additionally, as to the FE model can serve to benchmark approximate models, the FE result is compared with that of the Eckartina thick sediment case. The result indicates that the Eckart model can predict reflection loss with sound speed on the seafloor at a low grazing angle and with mean speed at a high grazing angle.

Furthermore, the multiple scattering effect on the sound field is considered. The total field is computed using the FE model under the shallow water environment. For the fluid case, the vertical coherence is strongly affected by the bottom scattering only in the short range scale because of the leaky mode attenuation. For the elastic case, the vertical coherence is dominated by the bottom scattering in the far range because of multiple scattering. For both cases, the longitudinal coherence has a much greater coherent length, and the longitudinal statistics are clearly shaped by modal interference lengths.

References

[1] Williams K L, Grochocinski J M and Jackson D R 2001 *J. Acoust. Soc. Am.* **110** 2956
[2] Yang T, Broschat S L and Galea C 2002 *IEEE J. Ocean. Eng.* **27** 403
[3] Thorsos E I 1988 *J. Acoust. Soc. Am.* **83** 78
[4] Soukup R J, Canepa G, Simpson H J, Summers J E and Gragg R F 2007 *J. Acoust. Soc. Am.* **122** 2551
[5] Gragg R F, Wurmser D and Gauss R C 2001 *J. Acoust. Soc. Am.* **110** 2878
[6] Tracey B H and Schmidt H 1999 *J. Acoust. Soc. Am.* **106** 2524
[7] Ivakin A N 1994 *Proceeding of the Third International Congress on Air-and Structure-Borne Sound and Vibration,* **3**, p. 1563
[8] Jackson D R, Odom R I, Boyd M L and Ivakin A N 2010 *IEEE J. Ocean. Eng.* **35** 603
[9] Isakson M J and Chotiros N P 2015 *IEEE J. Ocean. Eng.* **40** 475
[10] Bonomo A L, Isakson M J and Chotiros N P 2015 *J. Acoust. Soc. Am.* **137** EL235
[11] Jackson D and Richardson M 2007 *High-frequency seafloor acoustics* (New York: Springer Science & Business Media) pp. 475–482
[12] Ihlenburg F 1998 *Appl. Math. Sci.* **132** ch2
[13] Amestoy P, Duff I and L'Excellent J Y 2005 URL: http://mumps.enseeiht.fr
[14] COMSOL AB 2012 *COMSOL multiphysics user guide* (Version 4.3a)
[15] Berenger J P 1996 *IEEE Trans. on Antennas Propagation* **44** 110
[16] Zampolli M, Tesei A, Jensen F B, Malm N and Blottman J B 2007 *J. Acoust. Soc. Am.* **122** 1472
[17] Zampolli M, Jensen F B and Tesei A 2009 *J. Acoust. Soc. Am.* **125** 89
[18] Kapp D A 1995 "A new method to calculate wave scattering from rough surfaces at low grazing angles", Ph. D. Dissertation (Department of Mecharical Engeneering, Virginia Polytechnic State University, USA)
[19] Murray J and Ensberg D 1996 The swellex-96 experiment. URL: http://www.mpl.ucsd.edu/swellex96/
[20] Eckart C 1953 *J. Acoust. Soc. Am.* **25** 566
[21] Tracey B H 1996 An Integrated Modal Approach to Surface and Volume Scattering in Ocean Acoustic Waveguides (DTIC Document).
[22] Porter M B 1992 The KRAKEN normal mode program (DTIC Document)